

## Recovery of Equilibrium Free Energy from Nonequilibrium Thermodynamics with Mechanosensitive Ion Channels in *E. coli*

Uğur Çetiner<sup>1,2,3,\*</sup>, Oren Raz<sup>6</sup>, Sergei Sukharev<sup>1,2,3</sup> and Christopher Jarzynski<sup>1,2,4,5</sup>

<sup>1</sup>*Institute for Physical Science and Technology, University of Maryland, College Park, Maryland 20742, USA*

<sup>2</sup>*Maryland Biophysics Program, University of Maryland, College Park, Maryland 20742, USA*

<sup>3</sup>*Department of Biology, University of Maryland, College Park, Maryland 20742, USA*

<sup>4</sup>*Department of Chemistry and Biochemistry, University of Maryland, College Park, Maryland 20742, USA*

<sup>5</sup>*Department of Physics, University of Maryland, College Park, Maryland 20742, USA*

<sup>6</sup>*Department of Physics of Complex Systems, Faculty of Physics, Weizmann Institute of Science, Rehovot 7610001, Israel*



(Received 12 September 2019; accepted 21 April 2020; published 2 June 2020)

*In situ* measurements of the free energy difference between the open and closed states of ion channels are challenging due to hysteresis effects and inactivation. Exploiting recent developments in statistical physics, we present a general formalism to extract the free energy difference  $\Delta F$  between the closed and open states of mechanosensitive ion channels from nonequilibrium work distributions associated with the opening and closing of the channels (gating) in response to ramp stimulation protocols recorded in native patches. We show that the work distributions obtained from the gating of MscS channels in *E. coli* membrane satisfy the strong symmetry relation predicted by the Crooks fluctuation theorem. Our approach enables the determination of  $\Delta F$  using patch-clamp experiments, which are often inherently restricted to the nonequilibrium regime.

DOI: [10.1103/PhysRevLett.124.228101](https://doi.org/10.1103/PhysRevLett.124.228101)

**Introduction.**—Living cells in their native environments must cope with osmotic pressures arising from concentration gradients of osmolytes across the cytoplasmic membrane that separates the interior and exterior of the cell. When the cell's external medium undergoes abrupt dilution, the sudden rise in osmotic pressure draws water into the cell, which may lead to lethal membrane rupture (lysis). Mechanosensitive ion channels are biomolecular safety valves that the cell deploys in response to such osmotic shocks (see [1], Fig. S1). These channels typically exist in a closed state, but when the tension of the cytoplasmic membrane increases due to the influx of water, they open and the resulting outflow of osmolytes dissipates the excessive osmotic gradient. The channels reclose when tension returns back to normal.

In bacteria, the bulk release of osmolytes is primarily mediated by two families of channels: the mechanosensitive channels of small conductance (MscS, 1 nS) and of large conductance (3 nS). The latter open at large, near lytic tension, serving as a mechanism of last resort against extreme osmotic down shocks by forming wide, nonselective openings in the membrane [2,10,11]. The MscS channels, by contrast, open at lower tension and exhibit great diversity in structure and functionality [12,13].

To develop a quantitative physical understanding of mechanosensitive channels, it is crucial to obtain accurate measurements of their relevant properties. The free energy difference  $\Delta F$  between the open and closed states of a channel is an essential, path-independent thermodynamic

quantity characterizing the transition between these two states. A common method of determining  $\Delta F$  uses patch-clamp techniques to measure ion conductivity across the membrane as its tension is increased linearly in time until all the channels are open. These traces of conductivity vs tension reveal the probability of finding the channel in its open or closed state, and  $\Delta F$  is extracted by fitting this probability to a two-state Boltzmann distribution [2,3,11,14]. This method assumes that the ion channels remain in equilibrium during the tension ramping process. However, when a triangular ramp protocol is applied—increasing and then decreasing the tension at the same rate—one observes clear hysteresis, a hallmark of nonequilibrium behavior [15]. This hysteresis may explain the disparate estimates of  $\Delta F$  reported in the literature, ranging from  $5 k_B T$  to  $28 k_B T$  [4,16,17]. Evidently, the nonequilibrium character of experimental patch-clamp traces requires further analysis in order to extract accurate values of  $\Delta F$ .

Here, we investigate the thermodynamics of ion channel gating at the single-trajectory level and present an alternative approach of obtaining the free energy difference between the open and closed state of MscS, using recent developments in nonequilibrium statistical physics. In 1997, Jarzynski related the free energy difference between two equilibrium states of a system ( $A$ ,  $B$ ) to the nonequilibrium distribution of the work ( $W$ ) performed on the system during a thermodynamic process connecting  $A$  to  $B$  [18]

$$\langle e^{-\beta W} \rangle_{A \rightarrow B} = e^{-\beta \Delta F}. \quad (1)$$

Angular brackets denote an average taken over an ensemble of realizations of the same switching protocol starting from an equilibrium state ( $A$ ) in contact with a heat reservoir at temperature  $T$ , and  $\beta = 1/k_B T$  where  $k_B$  is the Boltzmann constant. In 1999, Crooks proved that the work distributions associated with the thermodynamic process of switching the system from  $A$  to  $B$  and with the corresponding time-reversed process from  $B$  to  $A$  satisfy the symmetry relation [19]

$$\frac{P_{A \rightarrow B}(W)}{P_{B \rightarrow A}(-W)} = e^{\beta(W - \Delta F)}. \quad (2)$$

These fluctuation theorems are robust with regard to how the microscopic dynamics are modeled [20–26] and have been experimentally verified in various systems [27–35]. Here, we show that nonequilibrium patch-clamp experiments can provide reliable estimates of the free energy difference between the open and closed states of ion channels.

We note that, except for the single-molecule “pulling experiments” performed through the application of linear force [20,27,29], in essentially all other systems, fluctuation theorems were used, not as a tool to extract quantities of interest, but rather to provide experimental verification of the theory. Our setup implements an entirely different experimental scenario where repeated application of tension to a membrane of live bacteria produces current traces that are interpretable using the fluctuation theorems, allowing us to determine  $\Delta F$  and to characterize dissipation during the functional cycle of a native mechanosensitive channel *in situ*. Here, we propose the first experimental design and analysis that provides a measure of how far from equilibrium the MscS channel performs its cycle under a relatively slow ( $\sim 1$ s) but commonly used stimulation regime. This analysis provides a reference point allowing us to project the amount of dissipated energy in “real-life” situations when a small bacterial cell swells in rainwater within  $\sim 10$  ms, and to assess how well mechanosensitive channels are optimized by a billion-year evolution to act as “emergency” release valves [36]. The problem of response speed and dissipation also directly pertains to voltage-gated channels where the movement of the voltage sensor domain always shows hysteresis [37]. Allosteric transitions in ligand-gated channels have been traditionally treated using thermodynamic cycles implying complete equilibria at every step [38], yet, in stark contrast, the measurements are usually performed in highly transient regimes (due to channel inactivation) raising the question of the validity of these equilibrium estimations. Here, we report the first adaptation of the conventional patch-clamp technique with fluctuation analysis that sheds light on nonequilibrium values of work, heat, and entropy production.

*Experimental and theoretical setup.*—The patch clamp technique developed by Neher and Sakmann in the late 1970s and early 1980s [39–41] enables researchers to characterize the conductive properties of individual ion channels by clamping a piece of a membrane as a gigaohm

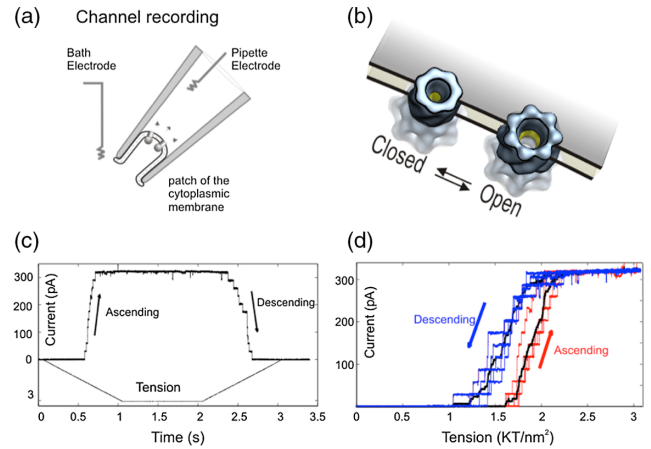


FIG. 1. (a) A micron-size glass pipette holds a cup-shaped patch separating the inside of the pipette from the bath. Suction stretches the curved patch membrane according to the law of Laplace, generating tension that activates the channels. The two electrodes measure the current reflecting the opening and closing transitions of individual channels. (b) A blowup of a fragment of the patch membrane showing two channels, in the closed and open states. The open channel has a larger cross-sectional area in the plane of the membrane. As membrane tension increases, the free energy of the open state decreases, making that state energetically more favorable. (c) A sample trace of current vs time with tension stimulus shown below. The membrane tension was increased linearly at a rate  $r = 3 k_B T / \text{nm}^2 \text{ s}^{-1}$  until all the channels in the membrane opened, manifested as the saturation of the current. After 1 s of equilibration at  $3 k_B T / \text{nm}^2$ , the tension was decreased back to  $0 k_B T / \text{nm}^2$  at the same rate  $r$ . The ascending and descending legs of the trace show the opening and closing of 11 MscS channels. (d) Five representative traces from the same patch are plotted as functions of tension in order to emphasize that the single channel events are stochastic and the system displays hysteresis as demonstrated by the averaged traces (black curves).

seal in a polished glass micropipette [Fig. 1(a)]. The high resistance of the seal provides an electrical isolation of the patch from the rest of the membrane. However, conducting pathways can be generated by activation of mechanosensitive ion channels in response to applied tension. This activation can be monitored with picoamp precision. Observations of discrete currents passing through individual channels made the patch-clamp technique essentially the very first single-molecule technique.

In our experiments, the system of interest is the collection of mechanosensitive ion channels embedded in the *E. coli*'s inner membrane. The micropipette with the clamped membrane is immersed into a solution at room temperature, which serves as a thermal reservoir. The work parameter (defined below) is the membrane tension,  $\gamma$ , and the conjugate variable to the work parameter is the lateral protein area expansion,  $\Delta A$  [Fig. 1(b)]. The application of suction changes the pressure between the two sides of the membrane and, hence, varies its tension, which allows us to perform work on the system and lower the free energy

difference between the open and closed states. Thus, in the presence of external tension on the membrane, states with larger area become favorable [2,42].

A typical experimental protocol starts with a membrane without any tension in which all ion channels are in the closed state and the conductance is negligible. Then, a linear increase in the membrane tension to a value of about  $3 k_B T/\text{nm}^2$  in 1 s is applied. This tension is kept constant for another second to let the system relax to equilibrium. Then, the tension is decreased back to  $0 k_B T/\text{nm}^2$  at the same rate. Figure 1(c) displays a characteristic “staircase” response of the current to these tension protocols: each step of current increase (decrease) represents a single channel opening (closing) event. In Fig. 1(c), 11 mechanosensitive channels are open in the final equilibrium state. Note that the longer the membrane is exposed to high tension values such as  $3 k_B T/\text{nm}^2$ , the greater the chance that it ruptures. A 1 s holding period is a safe time scale both to reach equilibrium (assuming a relaxation time of a few milliseconds at  $3 k_B T/\text{nm}^2$ , see also [1]) and to obtain a few realizations before the seal is lost. Figure 1(d) shows five representative current traces of the same protocol applied on the same membrane. Even though the same protocol is employed, the channel gating fluctuates, i.e., the traces and work values differ from one realization to the next. As indicated by the average currents [black curves, Fig. 1(d)], the system displays clear hysteresis, hence, we cannot expect the distribution of open and closed states to follow the Boltzmann distribution, and we will resort to non-equilibrium fluctuation theorems to determine  $\Delta F$ .

We model MscS as a two-state system (open-closed), and introduce a state variable,  $\sigma$ , which is 0 for a closed channel and 1 for an open one. Let  $\epsilon_{\text{closed}}$  and  $\epsilon_{\text{open}}$  denote the energies of the closed and open states. In the presence of tension  $\gamma$ , the energy of the system can be written as [43,44]

$$H(\sigma, \gamma) = H_0(\sigma) - \gamma A(\sigma), \quad (3)$$

where  $H_0(\sigma) = (1 - \sigma)\epsilon_{\text{closed}} + \sigma\epsilon_{\text{open}}$  represents the energy of the system due to the state of the ion channel alone, and the additional term  $\gamma A(\sigma) = \gamma\sigma\Delta A$  represents the energy difference between open and closed channels in the presence of tension, where  $\Delta A$  is the area difference between the closed and open states of the channel. Equation (3) omits a term  $f(\gamma)$ , representing the tension-dependence of the membrane energy, which contributes an additive offset  $f(\gamma_\tau) - f(\gamma_0)$  to both the free energy difference and the work, defined below (see the Supplemental Material [1] for full details).

For one realization of an experimental protocol of duration  $\tau$ , the work performed on the system is given by

$$W \equiv \int_0^\tau \dot{\gamma} \frac{\partial H}{\partial \gamma} dt = -\Delta A \int_0^\tau \dot{\gamma} \sigma dt. \quad (4)$$

(See [45,46] for a detailed discussion of this and alternative definitions of work.) It is convenient to rewrite Eq. (4) as a

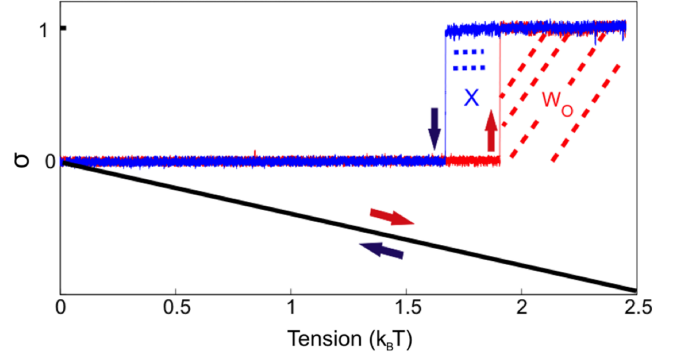


FIG. 2. The opening (red) and closing (blue) of a single channel in response to linear increase and decrease of the membrane tension with the same rate. By Eq. (5), the work performed during the opening is  $W_{C \rightarrow O} = -\Delta A \times W_0$  where  $W_0$  is the area under the red curve and the work performed during the closing is  $W_{O \rightarrow C} = \Delta A \times (W_0 + X)$  where  $(W_0 + X)$  is the area under the blue curve. The total dissipation for this cyclic process is  $W_{\text{diss}} = W_{C \rightarrow O} + W_{O \rightarrow C} = \Delta A \times X > 0$  which holds on average for small systems. The diagonal black line is the tension protocol and the dashed lines represent the areas under the corresponding curves.

sum, since the experimental acquisition yields digitized data in discrete time steps reflecting the sampling frequency

$$W = -\Delta A \sum_{k=0}^{M-1} (\gamma_{k+1} - \gamma_k) \sigma_{k+1}. \quad (5)$$

Here, the  $\gamma_k$ 's and  $\sigma_k$ 's are the values of the work parameter and the state of the system at the discrete time steps.

A typical realization for a cyclic protocol for an individual channel is depicted in Fig. 2 where the red curve represents the opening event and the blue curve is the closing event. In this case, for the ramp increase in the tension, Eq. (5) states that the work performed in order to open the channel,  $W_{C \rightarrow O}$ , is equal to  $-\Delta A \times W_0$  where  $W_0$  is the area under the red curve and the work performed during the closure,  $W_{O \rightarrow C}$ , is

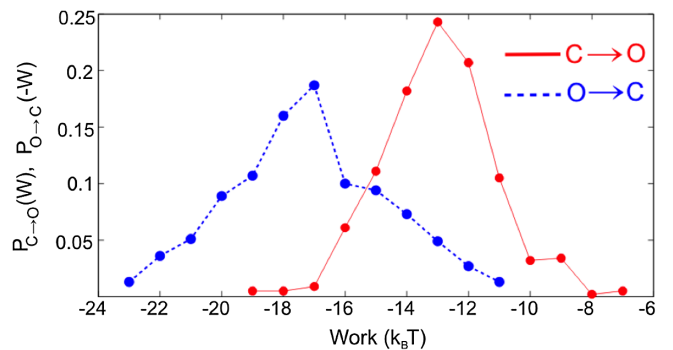


FIG. 3. Histograms of work distributions from 440 opening ( $C \rightarrow O$ ) and 449 closing ( $O \rightarrow C$ ) events. The protocol was performed time symmetrically at a rate  $r = 3 k_B T/\text{nm}^2 \text{ n}^{-1}$ , and work values were calculated using Eq. (5). The work distributions cross at  $-15.3 k_B T$ .



TABLE I. Summary of Results.  $\langle W \rangle_{\text{diss}} = \langle W \rangle_{C \rightarrow O} + \langle W \rangle_{O \rightarrow C}$  is the average dissipation during the cyclic process ( $C \rightarrow O \rightarrow C$ ). The various estimates of  $\Delta F$  discussed in the text are listed below, together with uncertainties calculated using the bootstrap method [47]. The uncertainty of  $\Delta F_0$  is different from  $\Delta F$  due to the boundary term and is obtained in [1] by error propagation. All quantities are given in units of  $k_B T$ .

$\langle W \rangle_{C \rightarrow O}$	$\sigma_{C \rightarrow O}$	$\langle W \rangle_{O \rightarrow C}$	$\sigma_{O \rightarrow C}$	$\langle W \rangle_{\text{diss}}$	$\Delta F_{\times}$	$\Delta F_C$	$\Delta F_{\text{OD}}$	$\Delta F_{\text{BAR}}$	$\Delta F_J$	$\Delta F_{\text{LR}}$
-13.0	1.82	17.2	2.60	$4.2 \pm 0.2$	$-15.3 \pm 0.6$	$-14.7 \pm 0.2$	$-14.7 \pm 0.2$	$-15.0 \pm 0.5$	$-14.5 \pm 0.3$	$-14.2 \pm 0.2$

equal to  $\Delta A \times (X + W_0)$  where  $X + W_0$  is the area under the blue curve and  $X$  is the area bounded by the two curves (see Fig. 2). The total dissipation during this thermodynamic cycle is positive, i.e.,  $W_{\text{diss}} = W_{C \rightarrow O} + W_{O \rightarrow C} = \Delta A \times X > 0$ . In other words, the typical work performed to open the channel is greater than that performed as the channel closes. However, in occasional realizations the thermal noise might act on the channel “constructively” and the channel might open at lower work values than the free energy difference,  $W < \Delta F$ , transiently violating the second law of thermodynamics.

*Results.*—An edge detection program was used to identify single channel events in all the traces (see [1], Fig. S2). The work distributions  $P_{C \rightarrow O}(W)$  and  $P_{O \rightarrow C}(-W)$ , obtained from over 800 individual opening and closing events in two independent experiments, are depicted in Fig. 3 with work values binned into 13 equal intervals. As described below and tabulated in Table I, we used these distributions to obtain various estimates of  $\Delta F$  based on Eqs. (1) and (2) as well as linear response theory.

By Eq. (2), the work distributions should cross at  $W = \Delta F$ , hence, we obtained an estimate of  $\Delta F_{\times} = -15.3 k_B T$  by finding the intersection of the measured work distributions. While convenient, this method is not optimal as it only uses local behavior of the work distributions around the crossing point. A better estimate,  $\Delta F_C = -14.7 k_B T$ , was obtained by fitting the plot of  $\log[P_{C \rightarrow O}(W)/P_{O \rightarrow C}(-W)]$  to a straight line and locating where it intercepts the work axis (see [1], Fig. S3A) [5,48]. Yet another estimate,  $\Delta F_{\text{OD}} = -14.7 k_B T$ , was constructed using the overlapping distributions (OD) method [5,48] (see [1], Fig. S4). All three of the above-mentioned methods use histograms of work values and, therefore, depend on the bin size. By contrast, Bennett’s acceptance ratio (BAR) method [5,49,50] yields an estimate  $\Delta F_{\text{BAR}} = -15.0 k_B T$  that is independent of bin size (see [1], Fig. S3B).

We also estimated  $\Delta F$  by applying Eq. (1) to both the closed  $\rightarrow$  open transition and to the open  $\rightarrow$  closed transition, obtaining  $-14.9 k_B T$  and  $-14.1 k_B T$ , respectively, yielding an average prediction  $\Delta F_J = -14.5 k_B T$  based on Eq. (1). Finally, linear response (LR) theory provides an estimate  $\Delta F = \langle W \rangle - \beta \sigma_W^2 / 2$  based on the mean and the variance of a work distribution [51]; applying this formula to both the opening and closing processes and then taking the average, we obtained  $\Delta F_{\text{LR}} = -14.2 k_B T$ .

Note that the estimates in Table I refer to the free energy difference between states associated with the initial and final values of the work parameter,  $\Delta F \equiv F(\gamma_\tau) - F(\gamma_0)$ . This quantity differs from the free energy difference between the closed and open states of the channel in the absence of any tension,  $\Delta F_0$ . The latter should be independent of the protocol and can be recovered from the former by adding the corresponding boundary term

$$\Delta F_0 = \Delta F + \gamma \sigma \Delta A|_0^\tau = -15 + 3 \times 12 = 21 k_B T. \quad (6)$$

Here, we chose Bennett’s estimate as our best guess for  $\Delta F$ . The final value of the tension is  $\gamma_\tau = 3 k_B T / \text{nm}^2$  and  $\Delta A$  was taken to be  $12 \text{ nm}^2$  based on the molecular dynamic simulation of crystallographic structures of the open and closed states of the channel [52] which is consistent with previous experimental studies (see [1] for error analysis) [3,4,6]. Using different techniques,  $\Delta F_0$  was determined to be  $22 \pm 1 k_B T$  [6].

*Discussion.*—We extracted the free energy difference between the closed and open states of a mechanosensitive ion channel in *E. coli*’s membrane from nonequilibrium work distributions obtained with the patch clamp setup where the work parameter is the membrane tension,  $\gamma$ , and the conjugate variable is the protein’s lateral area expansion,  $\Delta A$ . We used the electrical current through the membrane to infer the state of the channel, and Eq. (5) to obtain work values. Our estimators are in good agreement with one another and recover the free energy within  $k_B T$  of its best estimate obtained from an independent experiment (see also [1], Fig. S5). We consider Bennett’s acceptance ratio method as our most reliable estimate since it uses both the  $C \rightarrow O$  and  $O \rightarrow C$  work distributions, does not rely on binned histograms, and minimizes the variance of the estimate [5].

It is also worth mentioning that, even though the work parameter (the external tension) changes as a function of time according to a predefined protocol, in principle, it should not respond to the state of the system, namely, it should not fluctuate and should be identical in each realization of the protocol. This criterion can only be satisfied exactly in simulation or theory. This problem is not unique to our setup and appears, as well, in single molecule pulling experiments [53–55]. Care must be taken to ensure that the work parameter is properly chosen such that the fluctuations are negligible. In the Supplemental

Material [1], Fig. S6, we compared the work distributions and free energy difference obtained from two separate membranes having different number of MscS channels. Good reproducibility was observed among different membranes under the same protocol. Moreover, we tried a different protocol where the membrane tension was increased to  $3.6 k_B T/\text{nm}^2$  in 250 milliseconds giving a different  $\Delta F$ . As a control experiment, regardless of the final value of the work parameter or the rate,  $\Delta F_0$  should always be retrieved from Eq. (6) since the boundary term compensates for the difference in  $\Delta F$  (see [1], Fig. S7 and Table 2). Note that this process is more dissipative than the typical one-second experimental protocol—nearly  $8k_B T$  of work dissipated into the environment per cycle with a shorter and stronger tension ramp [1].

It is an experimental advantage to have as many channels as possible, since each single channel event yields an independent work value for every realization of the experimental protocol. Yet, many channels come with two complications inherent in all patch clamp experiments. (i) To use the proposed method, single channel events must be resolved. This becomes increasingly difficult when there are many channels in the same patch. Therefore, we expressed MscS in a tightly regulated pBAD (ThermoFisher) expression system which provided us a tight control of the protein expression level. (ii) If a channel changes its state more than once, the path it follows,  $\{\sigma_k; 0 \leq k \leq M\}$ , cannot be determined precisely for the rest of the protocol, since the single channel events are indistinguishable in the patch clamp setup. If such events, although not very common, happen in the beginning or at the end of the protocol, the error introduced will not be significant as shown in the Supplemental Material [1], Fig. S8. Despite this unavoidable complication, the patch clamp technique is still quite advantageous and offers fast convergence as sufficient statistics for the work distributions can be collected efficiently.

In conclusion, the presented measurements on the bacterial channel MscS allowed us to establish a reliable protocol to extract the free energy of the closed-to-open transitions and quantify the dissipation. The work paves the road toward studies of dissipation in other channels.

U.C. acknowledges support from the Maryland Biophysics Program and by the U.S. Department of Education GAANN Mathematics in Biology Fellowship. O. R. is supported by a research grant from Mr. and Mrs. Dan Kane and the Abramson Family Center for Young Scientists. The work was supported by NIH Grants No. R21AI105655 and No. GM107652 to S.S. C.J. acknowledges financial support from the National Science Foundation (USA), under Grant No. DMR-1506969. U.C. thanks Ms. Stephanie Sansbury for cloning MscS into tightly-regulated pBAD for expression system and Dr. Andriy Anishkin for the illustrations. U. C. is also indebted to Dr. Yiğit Subaşı for the stimulating discussions.

\*Department of Systems Biology, Harvard Medical School, Boston, MA 02115, USA.

- [1] See Supplemental Material at <http://link.aps.org/supplemental/10.1103/PhysRevLett.124.228101> for error analysis, experimental and theoretical details, which includes Refs. [2–9].
- [2] S. I. Sukharev, W. J. Sigurdson, C. Kung, and F. Sachs, Energetic and spatial parameters for gating of the bacterial large conductance mechanosensitive channel, *MscL*, *J. Gen. Physiol.* **113**, 525 (1999).
- [3] Y. Nakayama, K. Yoshimura, and H. Iida, Electrophysiological characterization of the mechanosensitive channel MscCG in *Corynebacterium glutamicum*, *Biophys. J.* **105**, 1366 (2013).
- [4] V. Belyy, K. Kamaraju, B. Akitake, A. Anishkin, and S. Sukharev, Adaptive behavior of bacterial mechanosensitive channels is coupled to membrane mechanics, *J. Gen. Physiol.* **135**, 641 (2010).
- [5] C. H. Bennett, Efficient estimation of free energy differences from Monte Carlo data, *J. Comput. Phys.* **22**, 245 (1976).
- [6] U. Çetiner, A. Anishkin, and S. Sukharev, Spatiotemporal relationships defining the adaptive gating of the bacterial mechanosensitive channel MscS, *Eur. Biophys. J.* **47**, 663 (2018).
- [7] K. Kamaraju, V. Belyy, I. Rowe, A. Anishkin, and S. Sukharev, The pathway and spatial scale for MscS inactivation, *J. Gen. Physiol.* **138**, 49 (2011).
- [8] P. Moe and P. Blount, Assessment of potential stimuli for mechano-dependent gating of MscL: Effects of pressure, tension, and lipid headgroups, *Biochemistry* **44**, 12239 (2005).
- [9] B. Martinac, M. Buechner, A. H. Delcour, J. Adler, and C. Kung, Pressure-sensitive ion channel in *Escherichia coli*, *Proc. Natl. Acad. Sci. U.S.A.* **84**, 2297 (1987).
- [10] S. I. Sukharev, P. Blount, B. Martinac, F. R. Blattner, and C. Kung, A large-conductance mechanosensitive channel in *E. coli* encoded by *mscL* alone, *Nature (London)* **368**, 265 (1994).
- [11] C.-S. Chiang, A. Anishkin, and S. Sukharev, Gating of the large mechanosensitive channel *in situ*: Estimation of the spatial scale of the transition from channel population responses, *Biophys. J.* **86**, 2846 (2004).
- [12] C. D. Cox, Y. Nakayama, T. Nomura, and B. Martinac, The evolutionary ‘tinkering’ of MscS-like channels: Generation of structural and functional diversity, *Pflügers Arch.* **467**, 3 (2015).
- [13] H. R. Malcolm and J. A. Maurer, The mechanosensitive channel of small conductance (MscS) superfamily: Not just mechanosensitive channels anymore, *ChemBiochem* **13**, 2037 (2012).
- [14] E. Petrov, D. Palanivelu, M. Constantine, P. R. Rohde, C. D. Cox, T. Nomura, D. L. Minor, Jr., and B. Martinac, Patch-clamp characterization of the MscS-like mechanosensitive channel from *Silicibacter pomeroyi*, *Biophys. J.* **104**, 1426 (2013).
- [15] F. Ritort, C. Bustamante, and I. Tinoco, A two-state kinetic model for the unfolding of single molecules by mechanical force, *Proc. Natl. Acad. Sci. U.S.A.* **99**, 13544 (2002).

- [16] A. Kloda and B. Martinac, Mechanosensitive channels of bacteria and archaea share a common ancestral origin, *Eur. Biophys. J.* **31**, 14 (2002).
- [17] S. Sukharev, Purification of the small mechanosensitive channel of *Escherichia coli* (MscS): The subunit structure, conduction, and gating characteristics in liposomes, *Bio-phys. J.* **83**, 290 (2002).
- [18] C. Jarzynski, Nonequilibrium Equality for Free Energy Differences, *Phys. Rev. Lett.* **78**, 2690 (1997).
- [19] G. E. Crooks, Entropy production fluctuation theorem and the nonequilibrium work relation for free energy differences, *Phys. Rev. E* **60**, 2721 (1999).
- [20] G. Hummer and A. Szabo, Free energy reconstruction from nonequilibrium single-molecule pulling experiments, *Proc. Natl. Acad. Sci. U.S.A.* **98**, 3658 (2001).
- [21] T. Hatano and S.-i. Sasa, Steady-State Thermodynamics of Langevin Systems, *Phys. Rev. Lett.* **86**, 3463 (2001).
- [22] S. X. Sun, Equilibrium free energies from path sampling of nonequilibrium trajectories, *J. Chem. Phys.* **118**, 5769 (2003).
- [23] D. J. Evans, A non-equilibrium free energy theorem for deterministic systems, *Mol. Phys.* **101**, 1551 (2003).
- [24] H. Oberhofer, C. Dellago, and P. L. Geissler, Biased sampling of nonequilibrium trajectories: Can fast switching simulations outperform conventional free energy calculation methods?, *J. Phys. Chem. B* **109**, 6902 (2005).
- [25] A. Imparato and L. Peliti, Work distribution and path integrals in general mean-field systems, *Europhys. Lett.* **70**, 740 (2005).
- [26] U. Seifert, Entropy Production Along a Stochastic Trajectory and an Integral Fluctuation Theorem, *Phys. Rev. Lett.* **95**, 040602 (2005).
- [27] J. Liphardt, S. Dumont, S. B. Smith, I. Tinoco, and C. Bustamante, Equilibrium information from nonequilibrium measurements in an experimental test of Jarzynski's equality, *Science* **296**, 1832 (2002).
- [28] F. Douarche, S. Ciliberto, A. Petrosyan, and I. Rabbiosi, An experimental test of the Jarzynski equality in a mechanical experiment, *Europhys. Lett.* **70**, 593 (2005).
- [29] D. Collin, F. Ritort, C. Jarzynski, S. B. Smith, I. Tinoco, Jr., and C. Bustamante, Verification of the crooks fluctuation theorem and recovery of RNA folding free energies, *Nature (London)* **437**, 231 (2005).
- [30] W. Wang, S. S. Black, M. D. Edwards, S. Miller, E. L. Morrison, W. Bartlett, C. Dong, J. H. Naismith, and I. R. Booth, The structure of an open form of an *E. coli* mechanosensitive channel at 3.45 Å resolution, *Science* **321**, 1179 (2008).
- [31] V. Blickle, T. Speck, L. Helden, U. Seifert, and C. Bechinger, Thermodynamics of a Colloidal Particle in a Time-Dependent Nonharmonic Potential, *Phys. Rev. Lett.* **96**, 070603 (2006).
- [32] N. C. Harris, Y. Song, and C.-H. Kiang, Experimental Free Energy Surface Reconstruction from Single-Molecule Force Spectroscopy Using Jarzynski's Equality, *Phys. Rev. Lett.* **99**, 068101 (2007).
- [33] O.-P. Saira, Y. Yoon, T. Tanttu, M. Möttönen, D. V. Averin, and J. P. Pekola, Test of the Jarzynski and Crooks Fluctuation Relations in an Electronic System, *Phys. Rev. Lett.* **109**, 180601 (2012).
- [34] S. An, J.-N. Zhang, M. Um, D. Lv, Y. Lu, J. Zhang, Z.-Q. Yin, H. Quan, and K. Kim, Experimental test of the quantum Jarzynski equality with a trapped-ion system, *Nat. Phys.* **11**, 193 (2015).
- [35] S. Ciliberto, Experiments in Stochastic Thermodynamics: Short History and Perspectives, *Phys. Rev. X* **7**, 021051 (2017).
- [36] U. Çetiner, I. Rowe, A. Schams, C. Mayhew, D. Rubin, A. Anishkin, and S. Sukharev, Tension-activated channels in the mechanism of osmotic fitness in *Pseudomonas aeruginosa*, *J. Gen. Physiol.* **149**, 595 (2017).
- [37] R. Olcese, R. Latorre, L. Toro, F. Bezanilla, and E. Stefani, Correlation between charge movement and ionic current during slow inactivation in shaker k<sup>+</sup> channels, *J. Gen. Physiol.* **110**, 579 (1997).
- [38] A. Auerbach, Thinking in cycles: Mwc is a good model for acetylcholine receptor-channels, *J. Physiol.* **590**, 93 (2012).
- [39] E. Neher and B. Sakmann, Single-channel currents recorded from membrane of denervated frog muscle fibres, *Nature (London)* **260**, 799 (1976).
- [40] O. P. Hamill, A. Marty, E. Neher, B. Sakmann, and F. Sigworth, Improved patch-clamp techniques for high-resolution current recording from cells and cell-free membrane patches, *Pflügers Arch.* **391**, 85 (1981).
- [41] B. Sakmann and E. Neher, Patch clamp techniques for studying ionic channels in excitable membranes, *Annu. Rev. Physiol.* **46**, 455 (1984).
- [42] K. Kamaraju, P. A. Gottlieb, F. Sachs, and S. Sukharev, Effects of GsMTx4 on bacterial mechanosensitive channels in inside-out patches from giant spheroplasts, *Biophys. J.* **99**, 2870 (2010).
- [43] T. Ursell, *Bilayer Elasticity in Protein and Lipid Organization: Theory and Experiments in Model Systems* (VDM Publishing, Saarbrücken, 2009).
- [44] R. Phillips, J. Theriot, J. Kondev, and H. Garcia, *Physical Biology of the Cell* (Garland Science, New York, 2012).
- [45] J. Horowitz and C. Jarzynski, Comparison of work fluctuation relations, *J. Stat. Mech.* (2007) P11002.
- [46] C. Jarzynski, Comparison of far-from-equilibrium work relations, *C. R. Phys.* **8**, 495 (2007).
- [47] B. Efron, Bootstrap methods: Another look at the jackknife, in *Breakthroughs in Statistics* (Springer, New York, 1992), pp. 569–593.
- [48] D. Frenkel and B. Smit, *Understanding Molecular Simulation: From Algorithms to Applications* (Elsevier, San Diego, 2001), Vol. 1.
- [49] G. E. Crooks, Path-ensemble averages in systems driven far from equilibrium, *Phys. Rev. E* **61**, 2361 (2000).
- [50] M. R. Shirts, E. Bair, G. Hooker, and V. S. Pande, Equilibrium Free Energies from Nonequilibrium Measurements Using Maximum-Likelihood Methods, *Phys. Rev. Lett.* **91**, 140601 (2003).
- [51] J. Hermans, Simple analysis of noise and hysteresis in (slow-growth) free energy simulations, *J. Phys. Chem.* **95**, 9029 (1991).
- [52] A. Anishkin, K. Kamaraju, and S. Sukharev, Mechanosensitive channel MscS in the open state: Modeling of the transition, explicit simulations, and experimental

- measurements of conductance, *J. Gen. Physiol.* **132**, 67 (2008).
- [53] M. Manosas and F. Ritort, Thermodynamic and kinetic aspects of RNA pulling experiments, *Biophys. J.* **88**, 3224 (2005).
- [54] J.-D. Wen, M. Manosas, P. T. Li, S. B. Smith, C. Bustamante, F. Ritort, and I. Tinoco, Jr., Force unfolding kinetics of RNA using optical tweezers. i. Effects of experimental variables on measured results, *Biophys. J.* **92**, 2996 (2007).
- [55] M. Manosas, J.-D. Wen, P. T. Li, S. B. Smith, C. Bustamante, I. Tinoco, Jr., and F. Ritort, Force unfolding kinetics of RNA using optical tweezers. ii. Modeling experiments, *Biophys. J.* **92**, 3010 (2007).